Introduction

Will incorporating a matching step into the ℓ_1 reformulation of EPSI [Lin and Herrmann, 2009] give better results than using EPSI alone, knowing that using EPSI one would match multiples to multiples instead of matching predicted multiplies to total data as in SRME?

To illustrate the potential benefit of adding curvelet-domain matching, let us consider a common-offset section from North Sea field dataset. Figure 1 indicates the results of primaries estimation from two different multiples-elimination methods, namely Surface-Related Multiple Elimination (SRME, Figure 1b), and Bayesian thresholding (Figure 1c, Saab et al. [2007]), which uses curvelet-domain matched-filtering. Comparing the primary estimations from SRME and Bayesian thresholding revels improved continuity and amplitude preservation for the primaries (near the lower two arrows in each plot around 2.6 and 3.1s) for primaries of the Bayesian thresholding method. Furthermore, the strong residual of the first- and second-order water bottom multiples in the shallow part (near the top two arrows in each plot around 0.75 and 1.2s) are better suppressed.

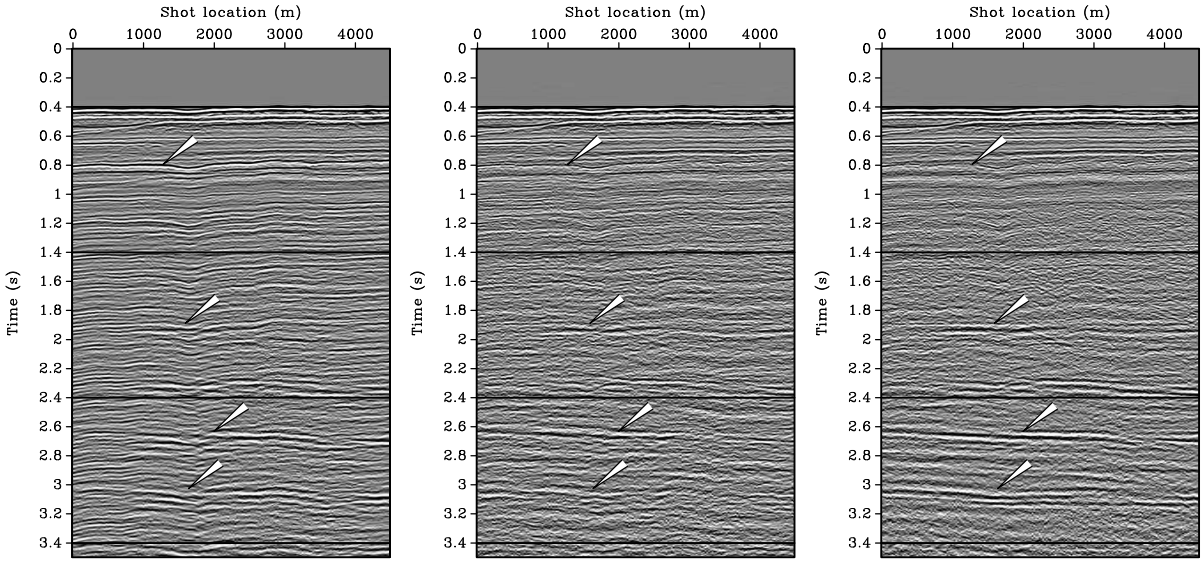

Figure 1: A common-offset section from North Sea field dataset with results from three different multiples elimination methods. **a)** Total data plotted with automatic-gain control. **b)** Primary estimation from one term SRME. **c)** Scaled Bayesian iterative thresholding primaries estimate. Partially adapted from Herrmann et al. [2008b].

Convexified EPSI

EPSI proposes an operator, based on the underlying principle that relates the primary impulse response to the total upgoing wavefield, which includes the source signature and surface-related multiples. EPSI monochromatic relationship is expressed mathematically as:

$$\underbrace{\hat{\mathbf{G}}}_{\text{surface-free impulse response}} \overbrace{\left[\hat{\mathbf{Q}} + \mathbf{R}\hat{\mathbf{P}}\right]}^{\text{downgoing wavefield}} \approx \overbrace{\hat{\mathbf{P}}}^{\text{upgoing wavefield}}, \tag{1}$$

where $\hat{\mathbf{G}}$ is the surface-free impulse response or the Green's function, $\hat{\mathbf{Q}}$ is the source signature, $\hat{\mathbf{P}}$ is the total upgoing wavefield, and $\mathbf{R}$ is the surface-reflectivity operator, which is approximated to $-\mathbf{I}$ with $\mathbf{I}$ the identity operator. The hat indicates a monochromatic representation of wavefields arranged into a matrix, see Berkhout [1985] for details. The matrix product of any two-hatted wavefields corresponds

to convolution in the time domain and a non-stationary convolution along the space coordinate.

Even though, the formulation of EPSI is original, its reliance on the zero norm makes it unstable and difficult to use in practice. Recent work by Lin and Herrmann [2009] addresses this important issue by reformulating EPSI in terms of a bi-convex optimization problem, where the surface-free Green's function is estimated by sparsity promoting and the wavelet is estimated by imposing Fourier domain smoothness. The starting point for this bi-convex inversion procedure is the following bi-linear forward model:

$$\mathbf{E}[\hat{\mathbf{Q}}]\mathbf{g} := \mathscr{F}_t^* \text{blockdiag}\left(\left[\hat{\mathbf{Q}} + \mathbf{R}\hat{\mathbf{P}}\right]_{1\cdots n_f}^* \otimes \mathbf{I}\right) \mathscr{F}_t \mathbf{g} = \mathbf{p}, \tag{2}$$

where $\mathbf{E}[\hat{\mathbf{Q}}]$ is a linear operator, which depends on the source signature $\mathbf{Q}$ and the upgoing wavefield $\mathbf{P}$ that acts on the vectorized surface-free Green's function $\mathbf{g}$, * denotes the conjugate transpose, and $\otimes$ denotes the Kronecker product. This expression reformulates the matrix-matrix product into a matrix-vector product. $\mathscr{F}_t$ is the Fourier transform, whose action on a vectorized wavefield $\mathbf{g}$ is defined as $\mathscr{F}_t\mathbf{g} := \hat{\mathbf{g}} = [\hat{\mathbf{g}}_1, \hat{\mathbf{g}}_2, \cdots, \hat{\mathbf{g}}_{n_f}]^*$ with n_f the number of frequencies and $\mathscr{F}_t^*$ is the inverse Fourier transform operator that brings the vectorized wavefield back to the time domain. The blockdiag lays out each frequency slice $(1\cdots n_f)$ in a vectorized form and $\mathbf{p}$ is the vectorized upgoing wavefield. For now, we will assume $\mathbf{R} = -\mathbf{I}$.

Equation (2) is linear in both the surface-free Green's function and the Fourier coefficients of the source function. This permits us to invert for these two unknowns by alternatingly solving two optimization problems, namely the one norm optimization problem on the unknown surface-free Green's function,

$$\widetilde{\mathbf{g}} = \arg\min_{\mathbf{g}} ||\mathbf{g}||_1 \quad \text{subject to} \quad ||\mathbf{p} - \mathbf{E}[\hat{\mathbf{Q}}]\mathbf{g}||_2 \leq \sigma, \tag{3}$$

where $\widetilde{\mathbf{g}}$ is the vectorized estimation (estimations are indicated by $\widetilde{\ }$) for the surface-free Green's function and σ is the residual, which is linked to the noise level of the data, and the regularized least-squares problem for the unknown source function,

$$\widetilde{\hat{\mathbf{q}}} = \arg\min_{\mathbf{q}} \frac{1}{2}||\widetilde{\mathbf{y}} - \mathbf{B}[\widetilde{\hat{\mathbf{G}}}]\hat{\mathbf{q}}||_2^2 + \lambda_F ||\mathbf{L}_F \hat{\mathbf{q}}||_2^2, \tag{4}$$

where $\widetilde{\mathbf{y}} = \text{vec}([\hat{\mathbf{P}} + \widetilde{\hat{\mathbf{G}}}\hat{\mathbf{P}}]_{1\cdots n_f})$ is the data vector with $\widetilde{\hat{\mathbf{G}}} = \text{vec}^{-1}(\widetilde{\mathbf{g}})$ the current estimate for the surface-free Green's function and $\mathbf{B}[\widetilde{\hat{\mathbf{G}}}] := \text{blockdiag}(\widetilde{\hat{\mathbf{G}}}_{1\cdots n_f} \otimes \mathbf{I})$. In this expression, we assume the source to be omnidirectional, i.e. $\mathbf{Q}_{1\cdots n_f} = \mathbf{I}q_{1\cdots n_f}$ The sharpening operator $\mathbf{L}_F$ in the ℓ_2 penalty term imposes smoothness on the estimated Fourier coefficients of the source function $\widetilde{\hat{\mathbf{q}}}$, which corresponds to enforcing decay in the time domain. The trade off parameter λ_F balances Fourier domain smoothness versus data misfit to avoid overfitting, which may lead to leakage of multiples into the source function.

In this bi-convex optimization, we start with estimate for the source function and then solve for the surface-free Green's function by an one-norm optimization problem, which seeks a sparse vector that after convolution with the downgoing wavefield explains the total upgoing wavefield, see Equation (3). Given this sparse estimation for the Green's function, the regularized least-squares problem is solved that seeks the Fourier coefficients of the source function, see Equation (4).

Curvelet-matched EPSI

Equation (4) corresponds to Fourier matching, which is also part of Surface Related Multiple Elimination. However, the difference is that the surface-free 'primaries' are matched to the total data instead of the predicted multiples as in SRME. This means that the output of Equation 4 produces estimates for the source wavelet and not its 'inverse'. With the appropriate choices for the regularization parameters, the above alternating optimization algorithm converges and produces reliable estimates for the surface-free data and the source function.

The success of EPSI hinges on the delicate relationship between the source wavelet and the upgoing total wavefield, on the one hand, and the surface-free impulse response on the other. EPSI leverages this relationship and this explains its success in solving the non-convex (read no global minimum) blind deconvolution problem where the source and surface-free impulse response are both unknown. However, this success comes at a price, namely a strict validity of this relationship. This means that we are implicitly assuming that the sources are omnidirectional and collocated, which can be accomplished relatively easily by proper regularization and extension of Fourier matching to include directivity; absence of 3D effects; infinite aperture; and ideal total reflection at the surface $\mathbf{R} = -\mathbf{I}$.

Unfortunately, these assumptions prove to be too restrictive in practice when data is not perfect as the example in Figure 1 shows. To address these issue, we follow the successful application of curvelet-domain matched-filtering during the SRME processing flow [Verschuur et al., 1992], we propose to incorporate this step in our methodology. This will allow us to mitigate possible adverse effects by correcting amplitude mismatches that vary smoothly as a function of position and dip along the predicted wavefronts of the current estimate for the surface-free impulse response. We correct for these errors by including a matching operator in the formulation—i.e., $\mathbf{R} \neq -\mathbf{I}$. This operator will be able to absorb amplitude errors of non-ideal reflections at the surface, finite-aperture, and other unknown effects.

We start by assuming $\mathbf{R}$ to be symmetric positive definite and pseudo local (no kinematic shifts). As in our earlier work on the curvelet-domain matched-filter [Herrmann, 2008], we model the amplitude errors—i.e., the operator $\mathbf{R}$—by a zero-order pseudodifferential operator, which can be interpreted as a space-dip-dependent filter. This operator can be approximated by a simple curvelet-domain scaling—i.e., we have

$$\mathbf{R} \approx \mathbf{C}^* \mathrm{diag}(\mathbf{z}) \mathbf{C}, \tag{5}$$

where $\mathbf{C}$ is the forward curvelet transform, $\mathbf{C}^*$ is its adjoint, which is also its pseudo inverse, and $\mathbf{z}$ is the curvelet-domain scaling vector. During curvelet-domain matched-filtering the diagonal in this expression is calculated by solving a regularized least-squares problem, possibly supplemented with a positivity constraint, i.e., $\mathbf{z} > 0$, during which the two wavefield are matched [Herrmann et al., 2008a].

by rearranging terms, we can extend the surface-free data estimation by incorporating Equation (5) into EPSI formulation Equation (2), yielding

$$\mathrm{vec}(\hat{\mathbf{P}} - \tilde{\hat{\mathbf{G}}}\tilde{\hat{\mathbf{Q}}}) = \hat{\mathbf{G}}\hat{\mathbf{M}}\mathbf{z}_{1\cdots n_s}, \tag{6}$$

where $\mathbf{M}_i = \mathbf{C}^* \mathrm{diag}(\mathbf{C}\mathbf{P}_i)$ with i the shot gather index and n_s is the number of sources. Our operator $\mathbf{R}$ now acts on each shot record of the upgoing wavefield $\mathbf{P}$ separately.

Incorporation of this expression into our formulation, yields a tri-convex optimization problem that now includes curvelet-domain matching.

$$\mathbf{z}_{1\cdots n_s} = \underset{\mathbf{z}_{1\cdots n_s}}{\arg\min} \frac{1}{2} ||\tilde{\mathbf{u}} - \mathbf{N}\mathbf{z}_{1\cdots n_s}||_2^2 + \lambda ||\mathbf{L}\mathbf{z}_{1\cdots n_s}||_2^2, \tag{7}$$

where $\mathbf{N} := \mathrm{blockdiag}([\tilde{\hat{\mathbf{G}}}\tilde{\hat{\mathbf{M}}}]_{1\cdots n_f} \otimes \mathbf{I})$ and $\tilde{\mathbf{u}} := \mathrm{vec}(\hat{\mathbf{P}} - \tilde{\hat{\mathbf{G}}}\tilde{\hat{\mathbf{Q}}})_{1\cdots n_f}$. The amount of smoothing is controlled by the parameter λ. For increasing λ, there is more emphasis on smoothness at the expense of overfitting the data, –i.e., erroneously fitting the primaries. The smoothness is promoted by the sharpening operator $\mathbf{L}$, which for each scale penalizes fluctuations amongst neighboring curvelet coefficients in the space and angle directions. See Herrmann et al. [2008a] for a detailed description.

Results

There are many factors that control the output of the matching process, e.g. the number of least-squares matching iterations and the amount of smoothness controlled by the parameter λ. These two parameters

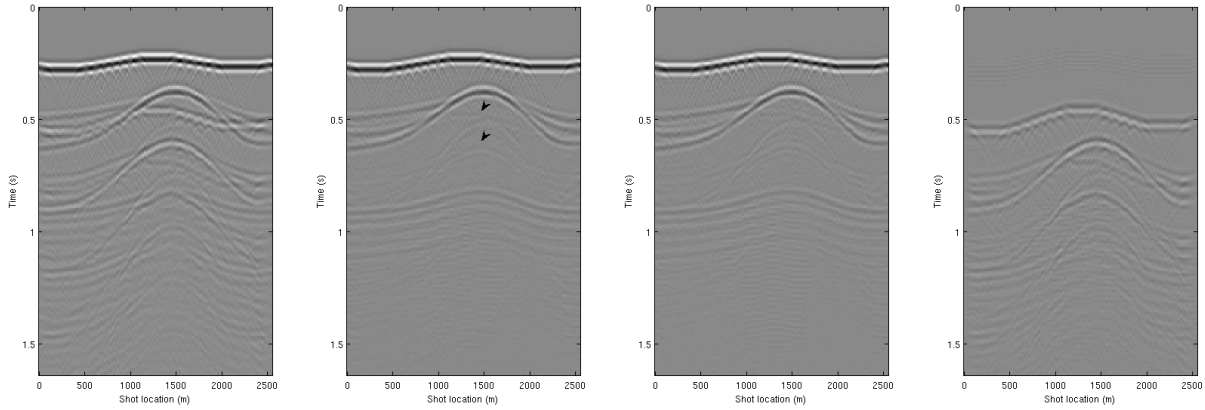

(a) (b) (c) (d)

Figure 2: Zero-offset EPSI synthetic data result with curvelet-domain matched-filtering incorporated once in the middle of the inversion process. The number of iterations is 60 and the regularization parameter $\lambda = 0.46$. **a)** Total upgoing wavefield section. **b)** Primaries estimation with matching. **c)** Primaries estimation without matching. **d)** primaries estimation minus the total data , i.e. the multiples estimate with matching.

control balance the smoothness and positivity of the curvelet-domain scaling versus data overfitting and long execution time. There is also the question of when and how frequent should we do the matching.

We conclude by comparing the result of EPSI with and without the curvelet-domain matching, Figure 2. The primaries estimate of EPSI with matching is better. The multiple event indicated by the top arrow is now weaker and more interestingly the other multiple indicated by the bottom arrow is no longer there. The matching was applied around the middle alternating optimization loop to give the best results since in that stage the inversion problem have already stabilized and the dramatic changes of the first few iterations have already done.

Acknowledgements

This work was in part financially supported by the Natural Sciences and Engineering Research Council of Canada Discovery Grant (22R81254) and the Collaborative Research and Development Grant DNOISE II (375142-08). This research was carried out as part of the SINBAD II project with support from the following organizations: BG Group, BP, Chevron, ConocoPhillips, Petrobras, Total SA, and WesternGeco.

References

Berkhout, A. [1985] *Seismic migration : imaging of acoustic energy by wave field extrapolation*. Elsevier.

Herrmann, F.J. [2008] Curvelet-domain matched filtering. *SEG Technical Program Expanded Abstracts*, SEG, vol. 27, 3643–3647.

Herrmann, F.J., Moghaddam, P.P. and Stolk, C.C. [2008a] Sparsity- and continuity-promoting seismic image recovery with curvelet frames. *Applied and Computational Harmonic Analysis*, **24**, 150–173, accepted for publication in the Journal of Applied and Computational Harmonic Analysis.

Herrmann, F.J., Wang, D. and Verschuur, D.J. [2008b] Adaptive curvelet-domain primary-multiple separation. *Geophysics*, **73**(3), A17–A21, doi:10.1190/1.2904986.

Lin, T. and Herrmann, F.J. [2009] Unified compressive sensing framework for simultaneous acquisition with primary estimation. *SEG*.

Saab, R., Wang, D., Yilmaz, O. and Herrmann, F. [2007] Curvelet-based primary-multiple separation from a bayesian perspective. *SEG International Exposition and 77th Annual Meeting*.

van Groenestijn, G.J.A. and Verschuur, D.J. [2009] Estimating primaries by sparse inversion and application to near-offset data reconstruction. *Geophysics*, **74**(3), A23–A28, doi:10.1190/1.3111115.

Verschuur, D.J., Berkhout, A.J. and Wapenaar, C.P.A. [1992] Adaptive surface-related multiple elimination. *Geophysics*, **57**, 1166–1177.